New Phytologist Supporting Information

Characterization of evolutionarily conserved key players affecting eukaryotic flagellar motility and fertility using a moss model

Rabea Meyberg, Pierre-François Perroud, Fabian B. Haas, Lucas Schneider, Thomas Heimerl, Karen S. Renzaglia, Stefan A. Rensing

Accepted: 7 February 2020

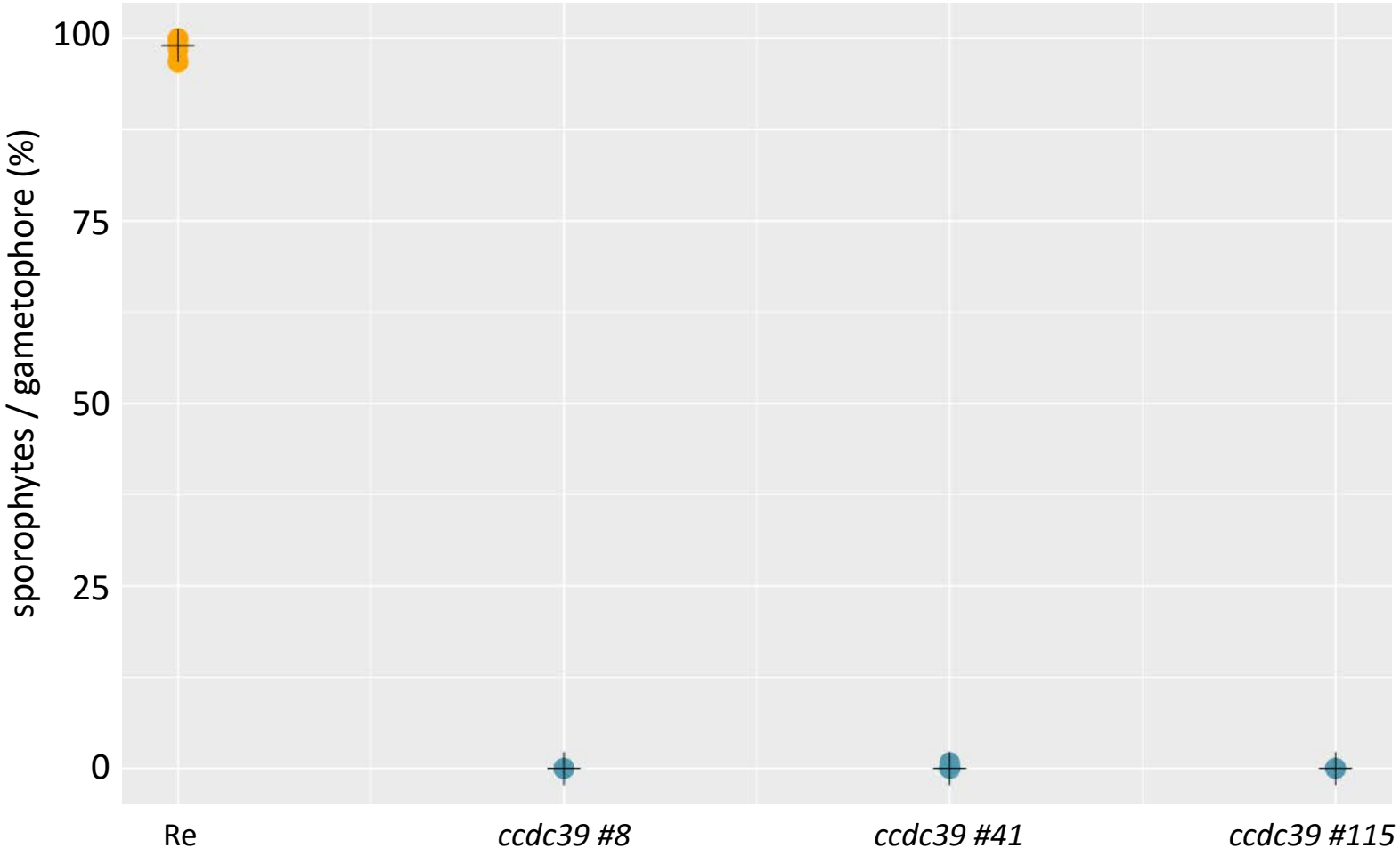

Figure S1: Sporophytes per gametophore developed under selfing conditions for all three independently analysed *ccdc39* strains.
All c*cdc39#8* (n = 546), *ccdc39#41* (n = 714) and *ccdc39#115* (n = 537) show in median 0% of sporophytes in comparison to median 99% of sporophytes for the corresponding wildtype background Re.

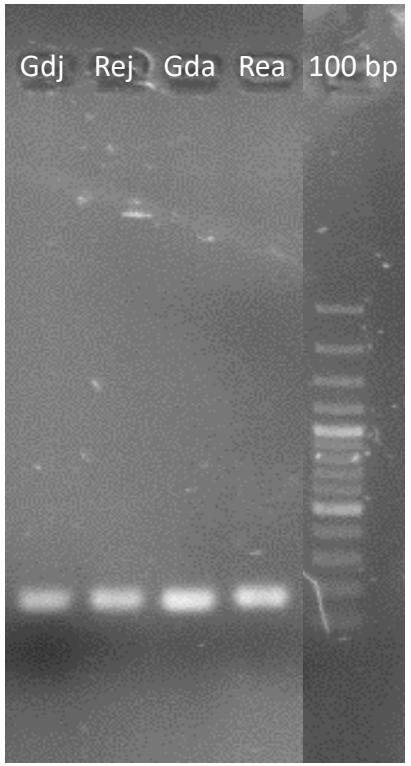

Figure S2: Expression level of act5 in juvenile (j) and adult (a) apices of Gd and Re are similar.

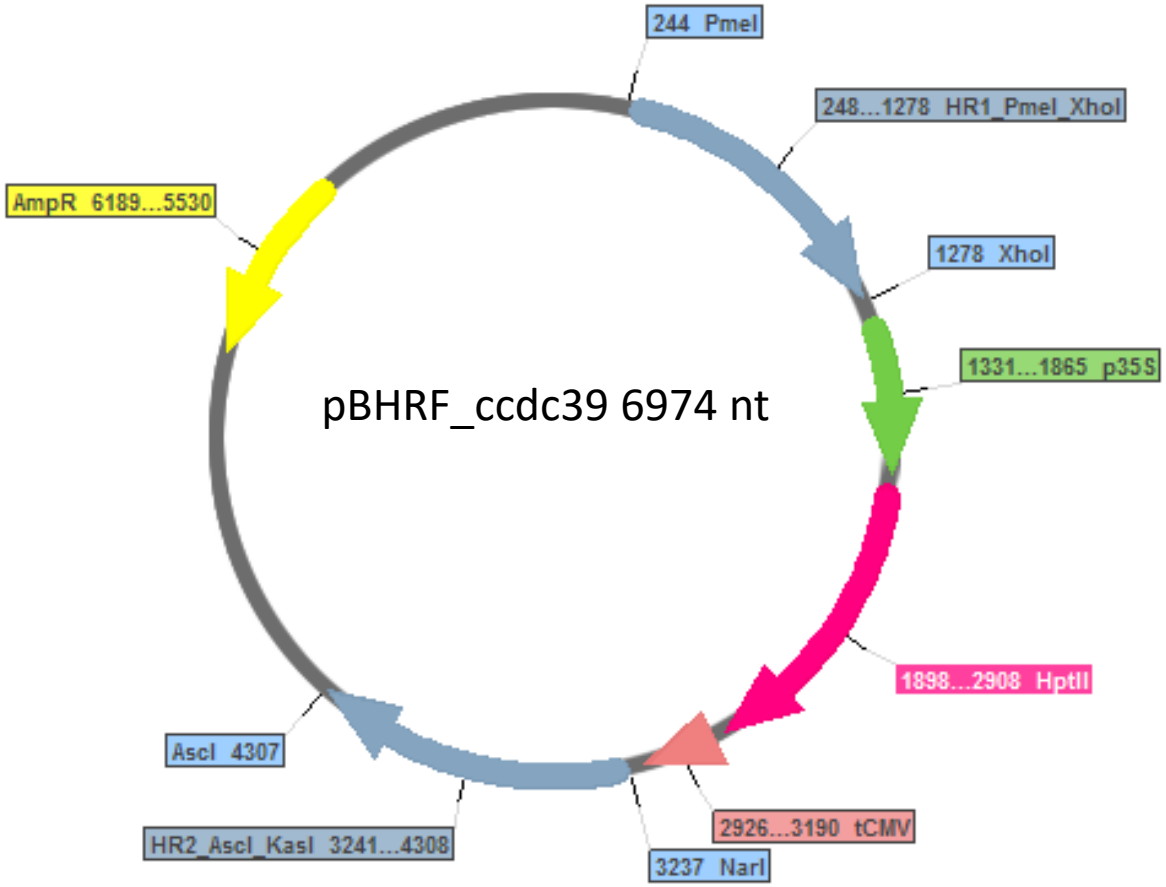

Figure S3: Final vector for amplification via ampicillin selection (yellow) of the knock out cassette flanked by the enzymes *Pme*I and *Asc*I. HR1 and HR2 (blue) flank the resistance cassette consisting out of the 35S promotor (green), the *hptII* resistance gene (pink) and the CMV terminator (red).

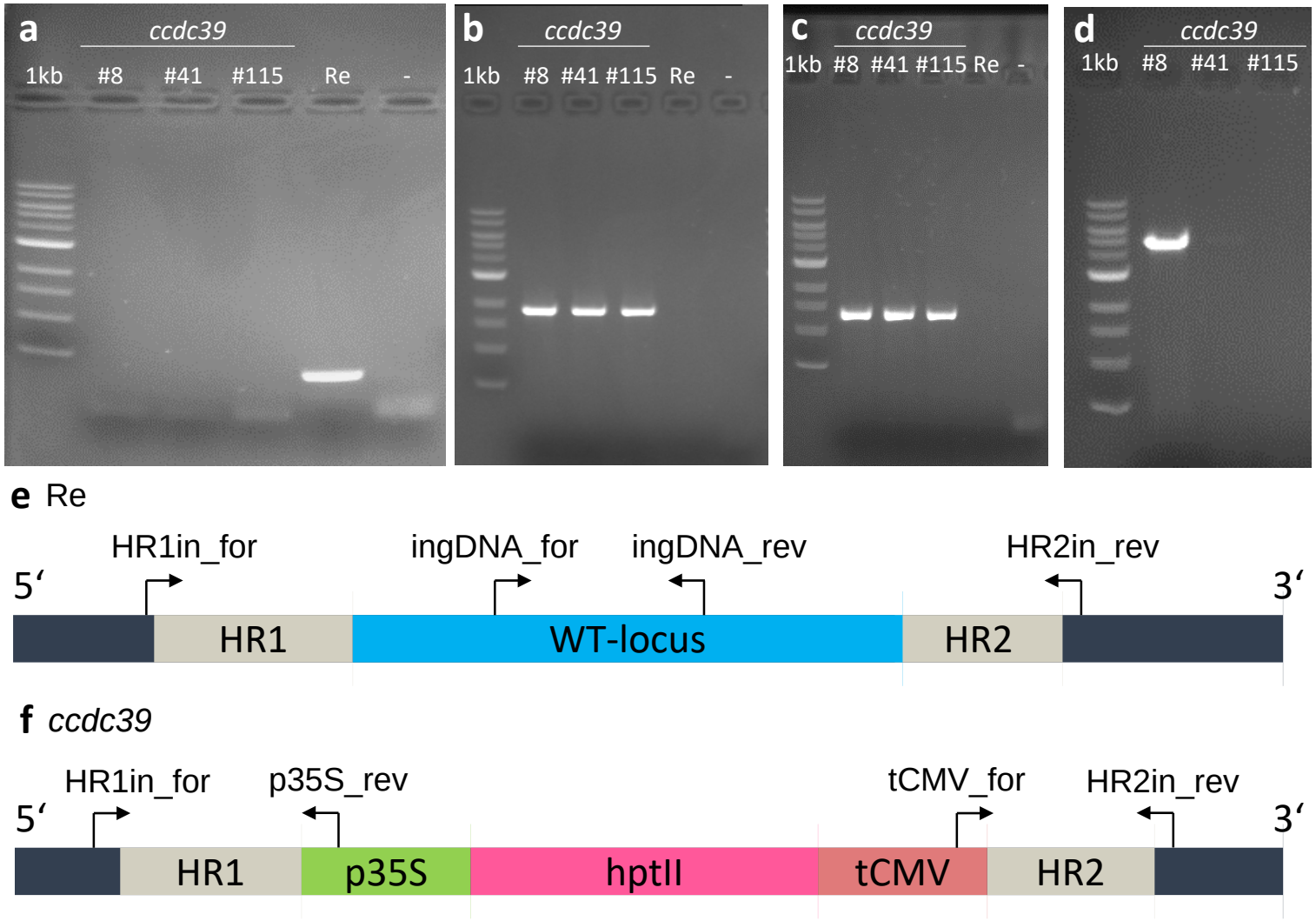

Figure S4: Gel images and sketch (E,F) of performed genotyping on Re and *ccdc39* gDNA.

Presence of the wild type locus was tested using ingDNA_for/rev (a). HR1 (b) and HR2 (c) presence was verified using HR1in_for/p35S_rev and tCMV_for/HR2in_rev. Full length amplification was performed using HR1in_for/HR2in_rev (d).

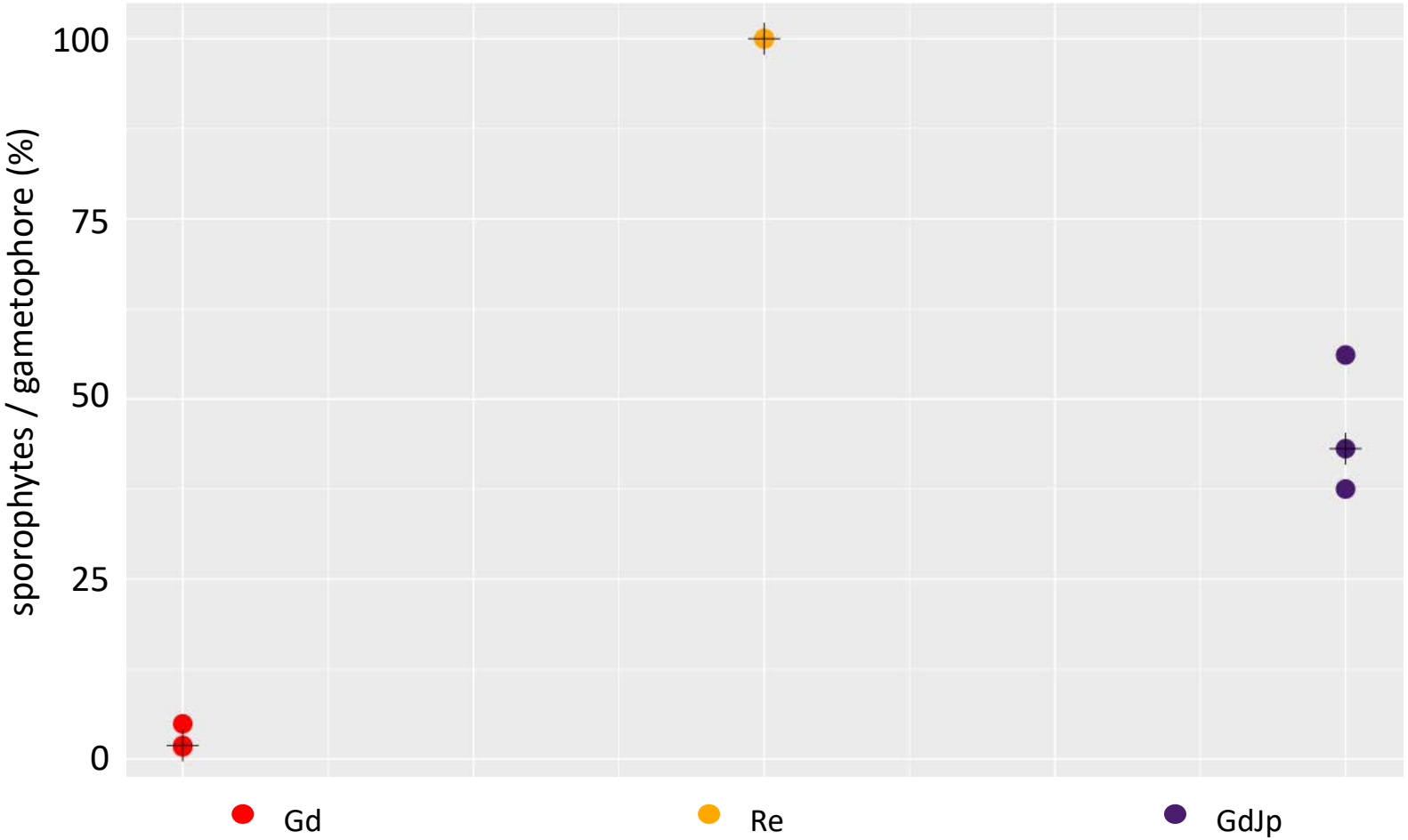

Figure S5: Number of sporophytes per gametophore developed under selfing conditions for *P. patens* ecotypes Re, Gd and GdJp.
Re (n = 3, 730 gametophores) shows median 100% sporophyte per gametophore, Gd (n = 3, 523 gametophores) shows 1.9% sporophytes per gametophore and GdJp (n = 3, 653 gametophores) 43.1%. GdJp develops significantly more sporophytes per gametophore in comparison with Gd ($p < 0.05$, t-test).

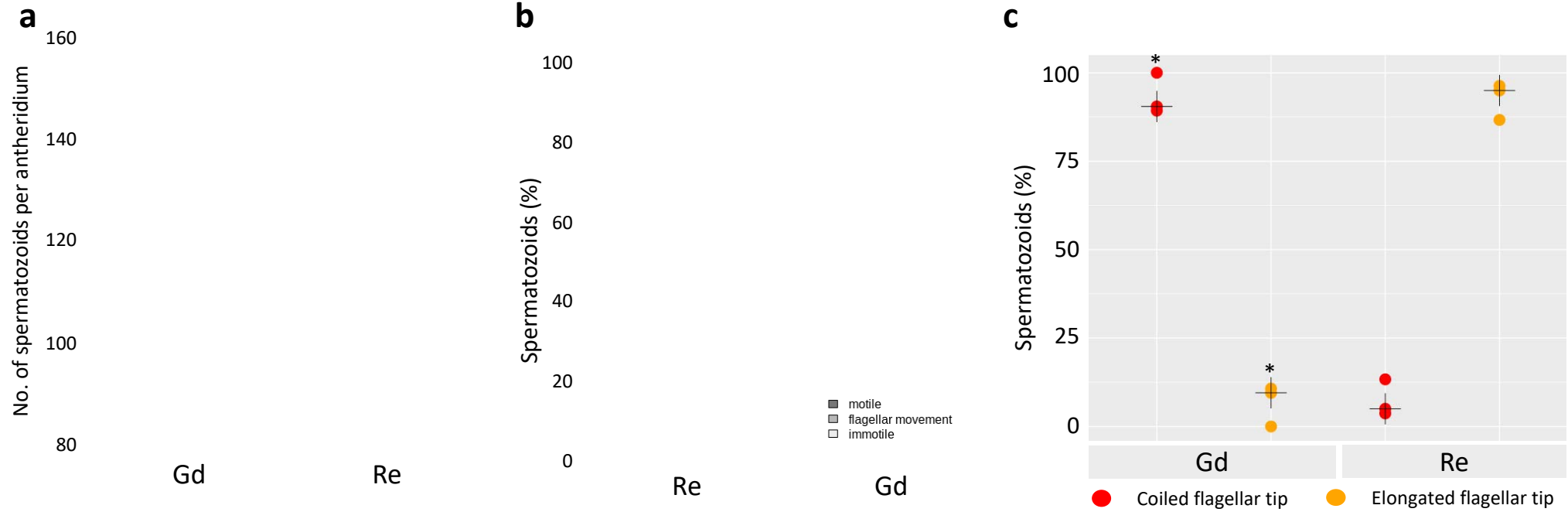

Figure S6: Detailed analysis of Gd and Re spermatozoids.
The number of spermatozoids per antheridium does not vary significantly between Gd and Re (a, n = 10 of each ecotype). Median-centered box-dotplots representing 50% of the measurements within the white box, whereas the whiskers show the 1.5 interquartile range (IQR). Dots show individual measurements. In Re, 94% of the spermatozoids were motile, 6% were immotile of which 3% showed flagellar movement. In Gd, 8% of the spermatozoids where motile, 92% were immotile, of which 24% showed flagellar movement. The number of motile spermatozoids is significantly different between ecotypes (b, Gd n = 50, Re n = 103, $p < 0.01$ chi-square test). c: Gd spermatozoids (n = 51) show coiled flagellar tips statistically significantly more often compared to Re spermatozoids (n = 62, $p < 0.01$, t-test). Median: black cross.

Figure S7: GO bias analysis and word cloud vizualization.

Over-represented terms are shown in green, whereas under-represented terms are shown in red. Larger font size correlates with a higher significance level. Genes affected by DMPs between Re and Gd in any of the contexts (CG, CHH, CHG) show over-representation of terms connected to cilia motility as well as terms related to macromolecule modification (a). Genes expressed in Gd (b) and Re (c) antheridia bundles show over-representation of polyamine and peptide biosynthetic processes as well as under-represented terms associated with mRNA capping.

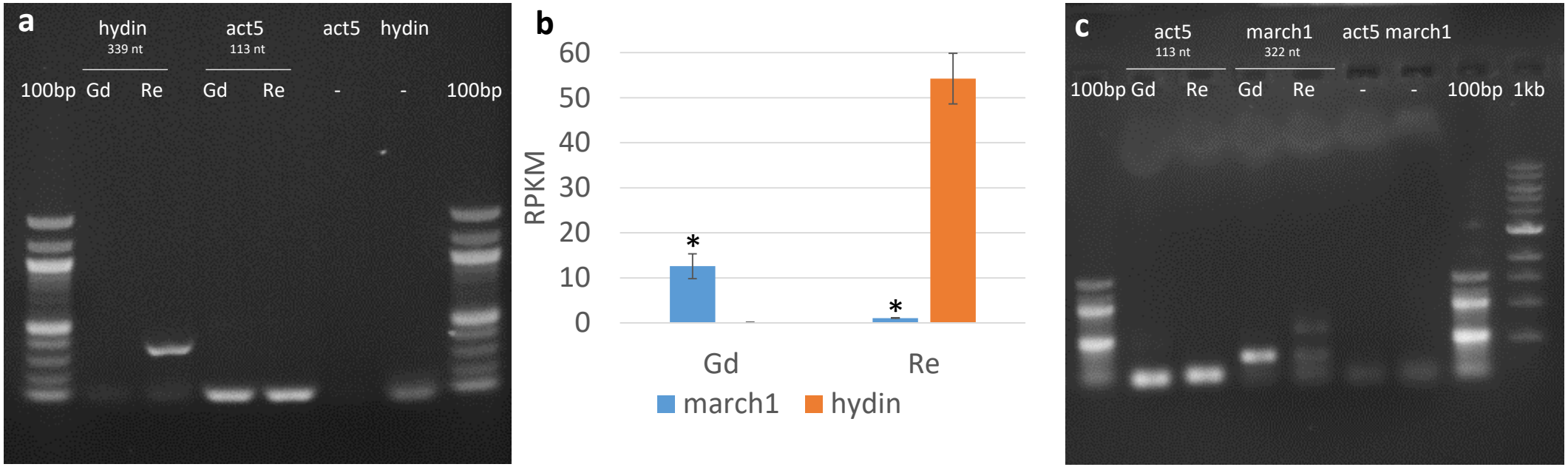

Figure S8: Expression analysis of genes expressed in antheridia bundles.
RT-PCR expression of hydin (a) and march1 (c) in adult gametophore apices of Gd and Re. Expression of hydin (339 nt) and march1 (322 nt) compared to the reference gene actin5 (113nt) genes matches RNA-seq data (b). Hydin shows no expression in the Gd but in the Re background, whereas march1 shows less expression in the Re background compared to Gd. b: RNA-seq expression of Gd and Re march1 (blue) and hydin (orange) show significant differences between Gd and Re (*, $p < 0.01$ t-test), error bars = +/- standard deviation, RPKM = reads per kilobase per million mapped reads.

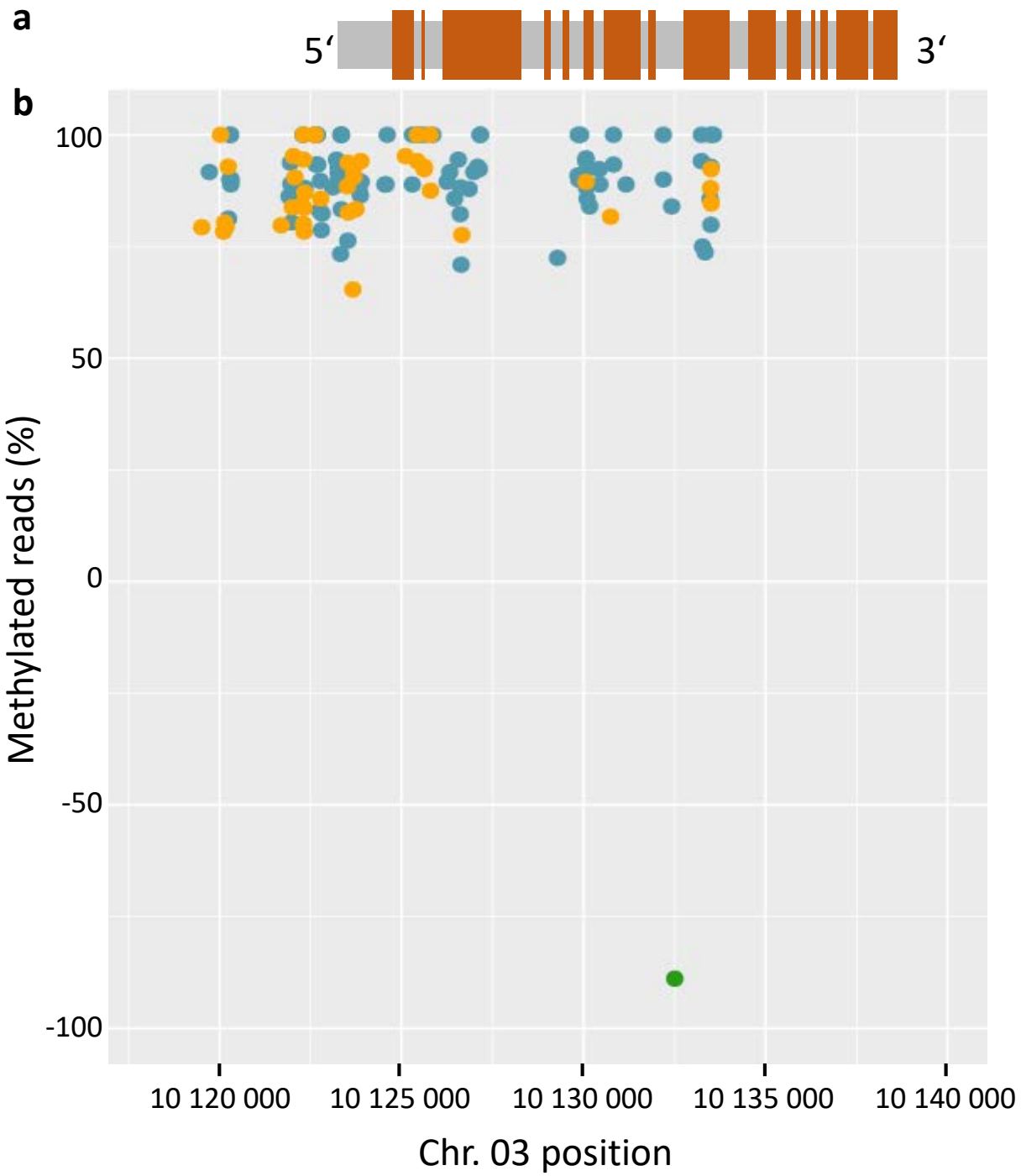

Figure S9: Methylation analysis of the hydin gene.
a: Exon and intron pattern of hydin. b: Aligned with the differentially methylated positions (DMPs) whereas 0 to 100 represents positions methyated with 0-100% in Gd and 0 to -100 represents positions methylated with 0-100% in Re. Gene body and 5‘-UTR of Gd hydin are highly affected by DNA methylation showing CHG (94, blue) and CHH (41, yellow) methylation, whereas in Re a single CG (green) methylation could be detected in an intron.

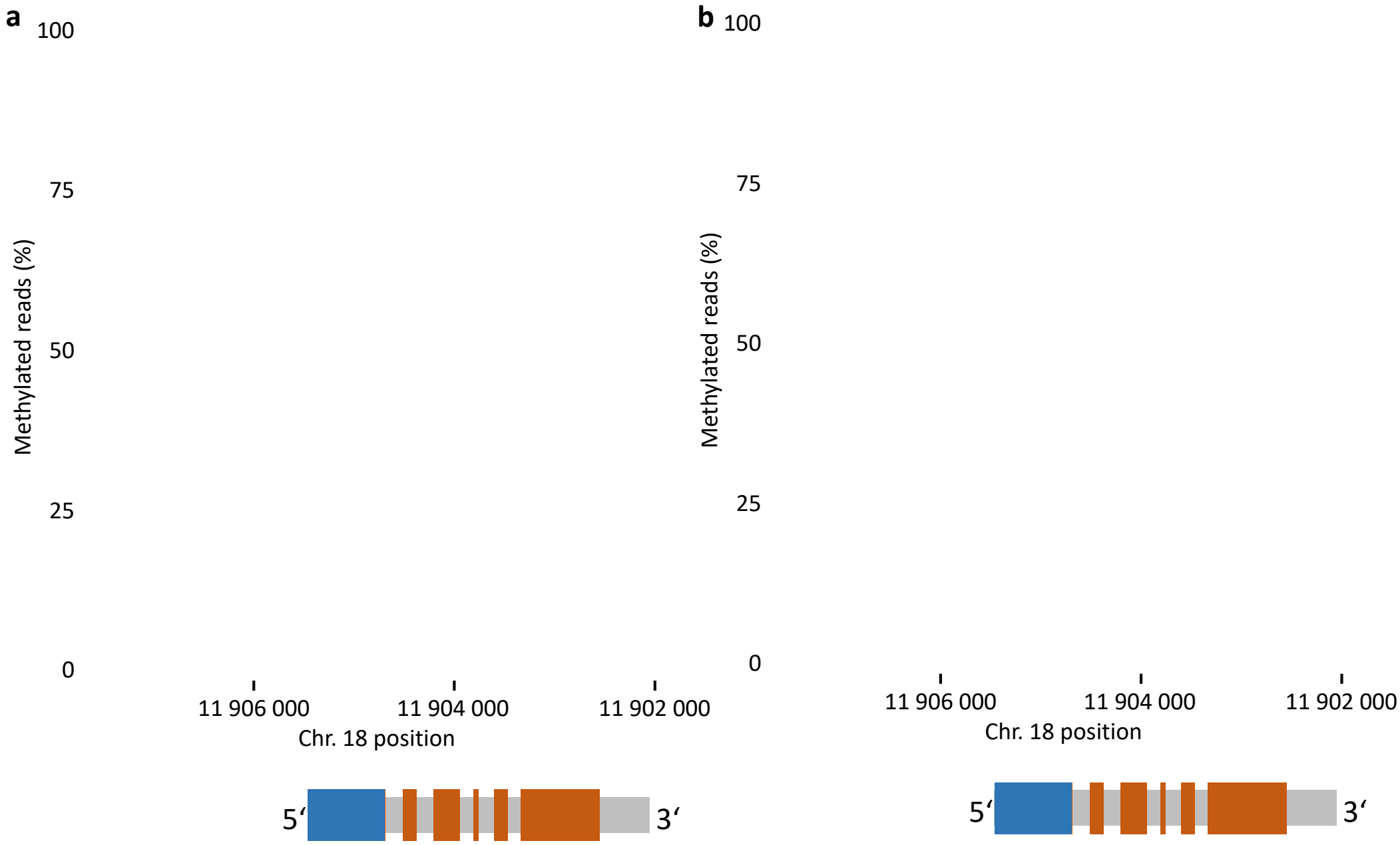

Figure S10: March1 gene body methylation. Percentage of methylated reads per position per pattern of Gd (a) and Re (b) adult gametophores. The V3.3 gene model of march1 is shown in grey, the UTRs are marked in blue and exons are shown in orange. Very low levels of methylation are detectable in march1 and 2kb upstream in both Gd and Re. CHG (blue), CHH (yellow) and CpG (green) marks are shown.

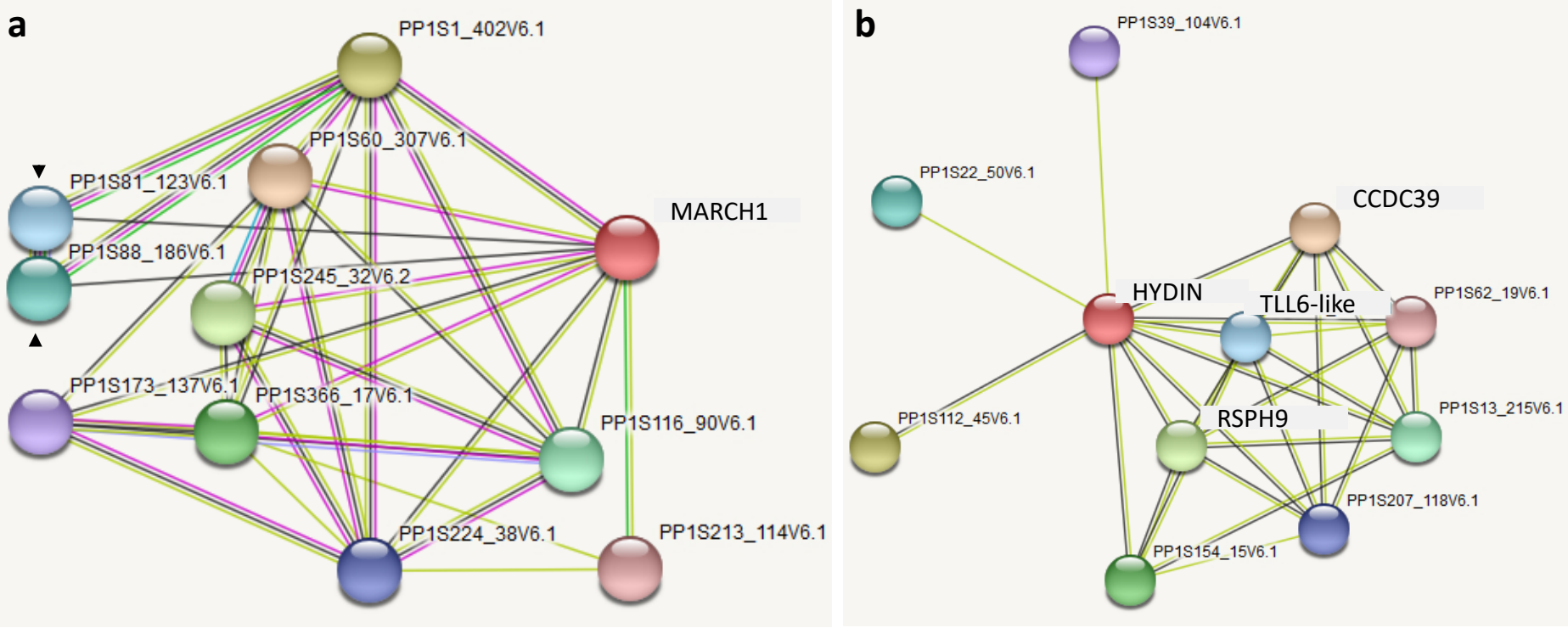

Figure S11: Network analysis of genes associated with proper flagellar function.
a: March1 network shows two protein phosphatases being co-expressed in common with CCDC39 (C, black arrows). b: Network analysis of hydin shows connectivity with genes affecting sperm cells (CCDC39, RSPH9, TLL6-like). c: Network analysis of CCDC39. Coexpressed protein phosphatases marked by black arrows. Line color specifies connection type between analysed proteins: dark grey marks co-expression, light green marks literature analysis, sky blue marks protein homology, grass green marks gene neighborhood, cyan marks interaction shown by curated databases, pink marks experimentally determined interactions.

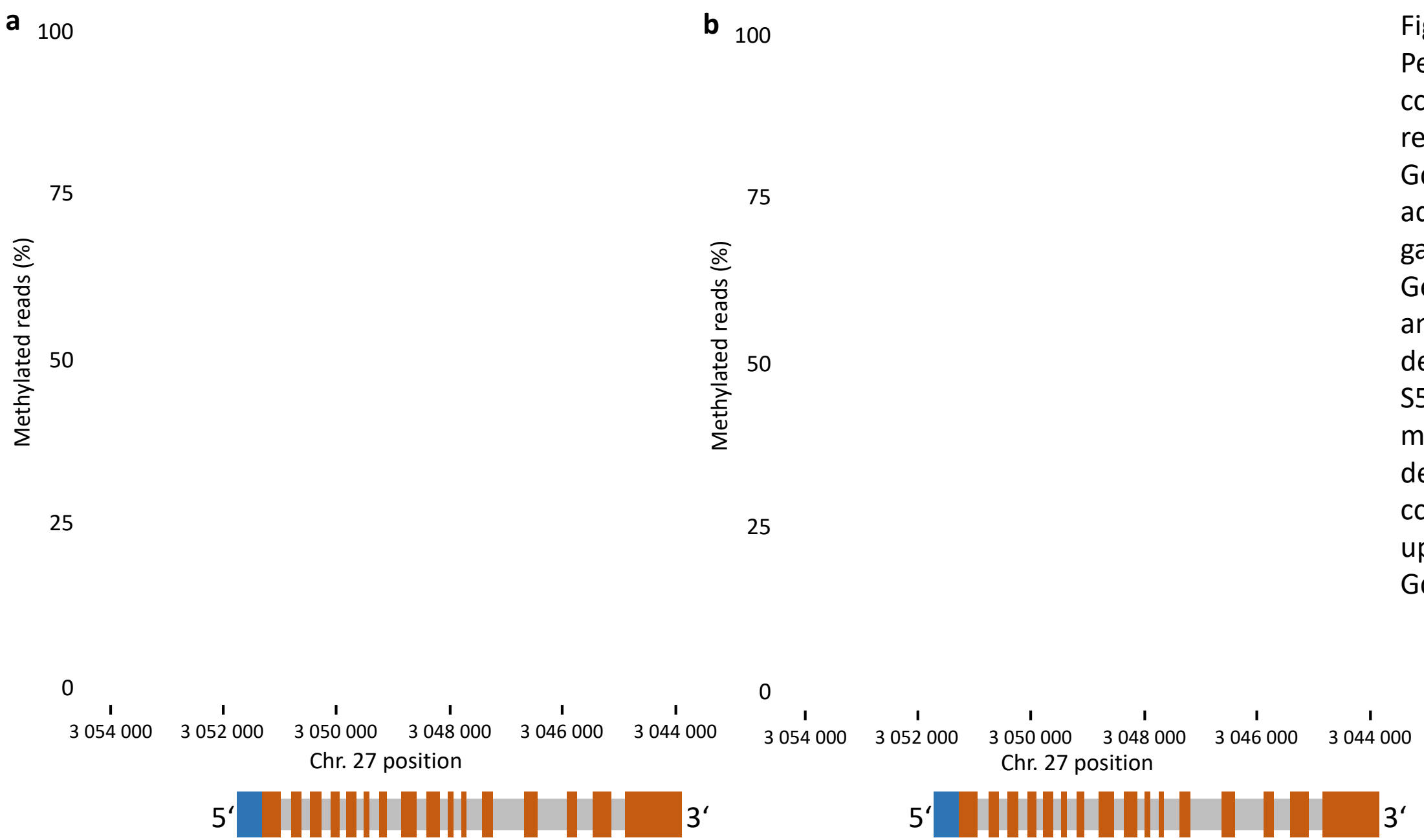

Figure S12: Percentage of ccdc39 methylated reads per position. Gd (a) and Re (b) adult gametophores. Gene model annotation as described in Fig. S5. Low gene body methylation is detectable in ccdc39 and 2kbp upstream in both Gd and Re.

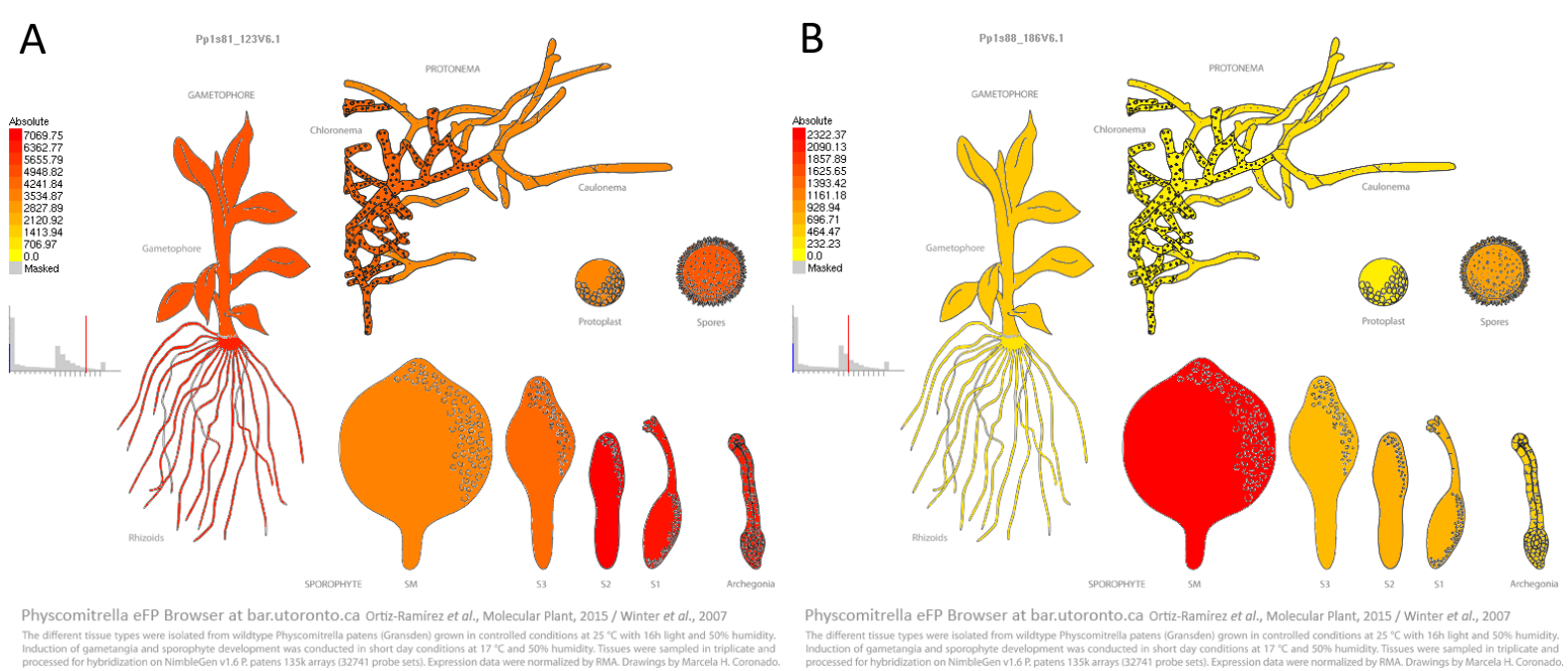

Figure S13: Expression of two cGMP kinases present in the ccdc39 and march1 network analysis. Both kinases show expression that is not restricted to sexual reproduction phases. Pp3c16_18360V3.1 (a) shows a broad expression in nearly every tissue with a focus towards the early sexual reproductive tissues, whereas Pp3c25_7050V3.1 (b) is highly expressed in mature sporophytes and shows only moderate to low expression in the other stages (error bars = +/- standard deviation). c: Both kinases show expression in antheridia bundles. a,b: Data from Ortiz-Ramirez *et al.*, 2016.

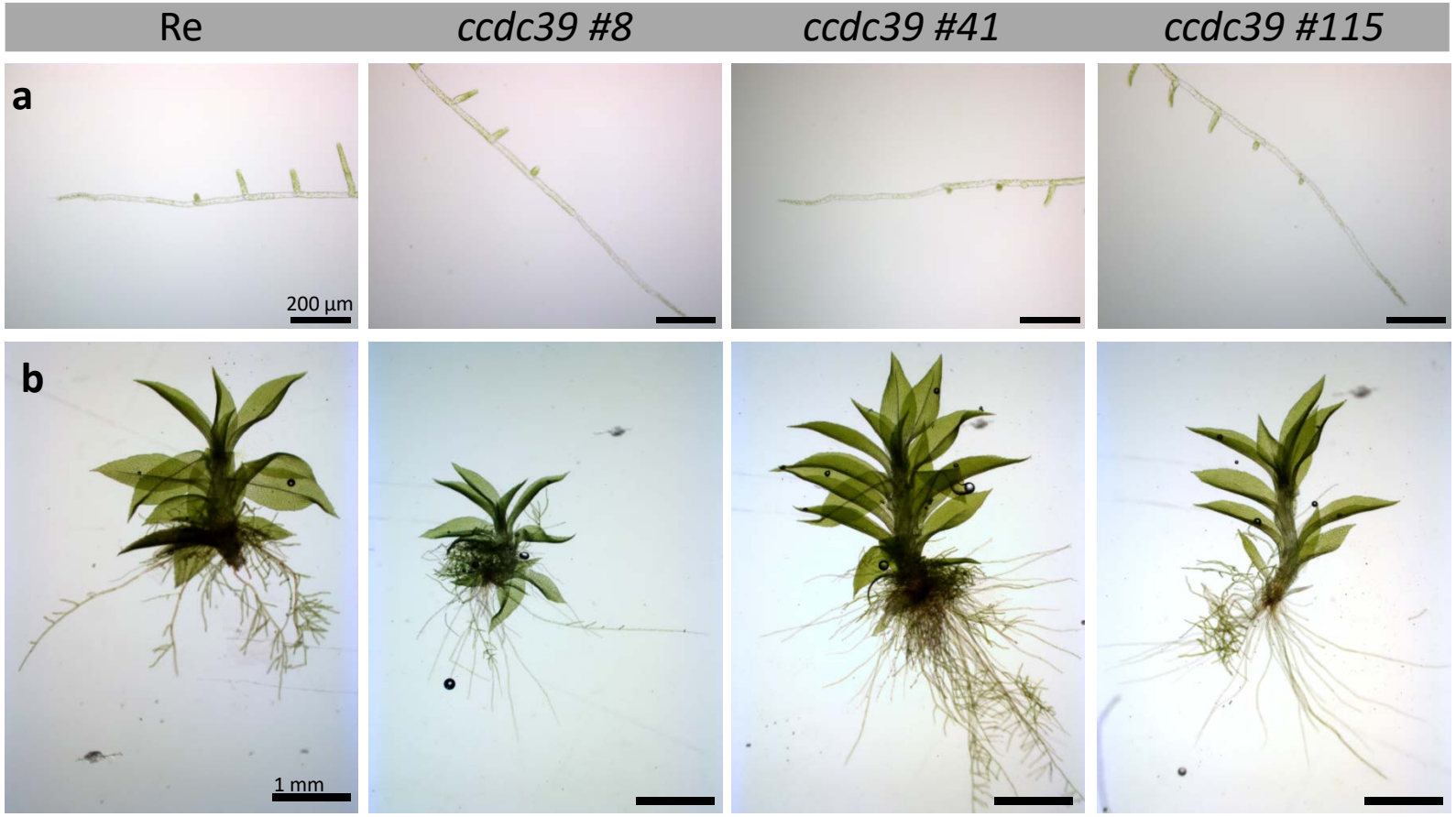

Figure S14: Protonema (a) and gametophore (b) development of Re compared to *ccdc39* mutant strains.
No obvious morphological differences could be observed in the analysed mutant lines.

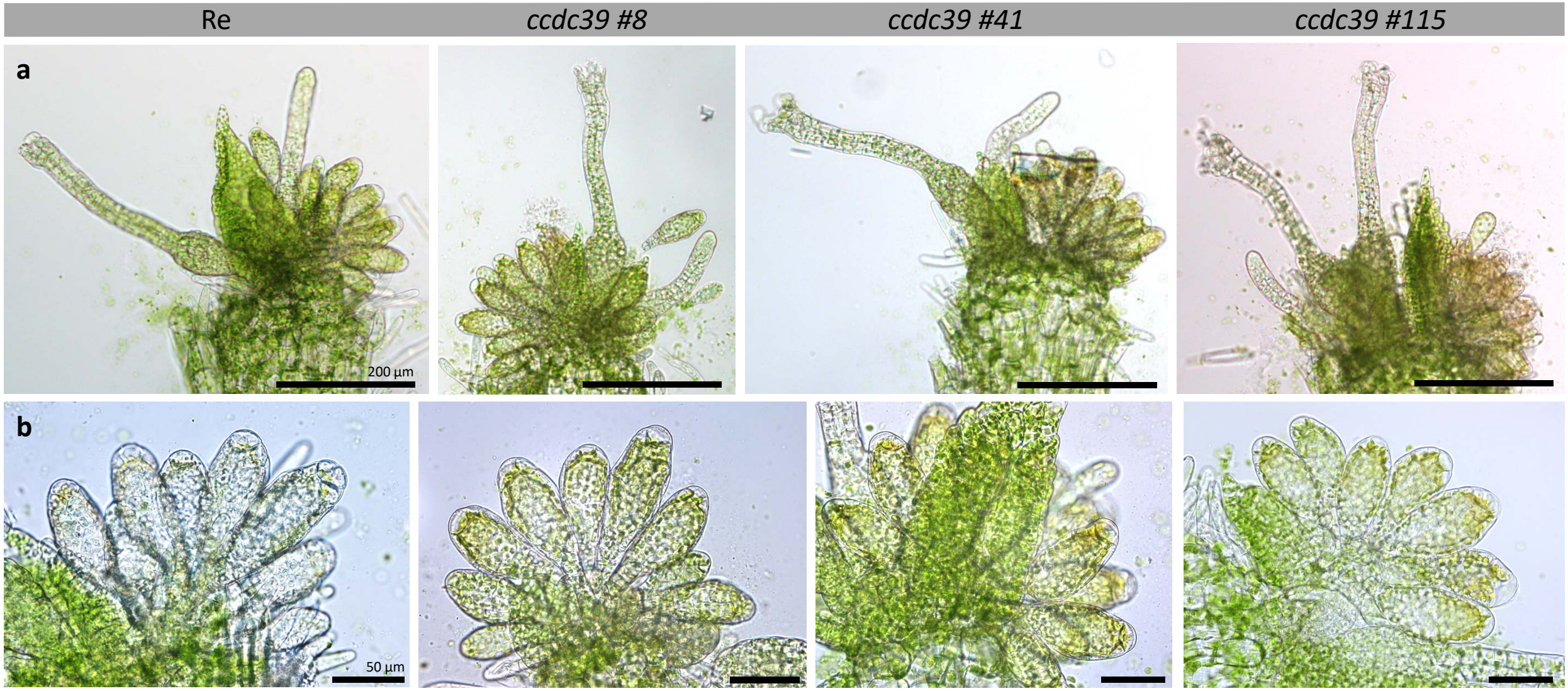

Figure S15: Gametangia development of *ccdc39* mutant strains compared to Re.
No obvious morphological differences can be detected. a: dissected apices with both archegonia and antheridia, b: detailed images of the antheridia bundles.

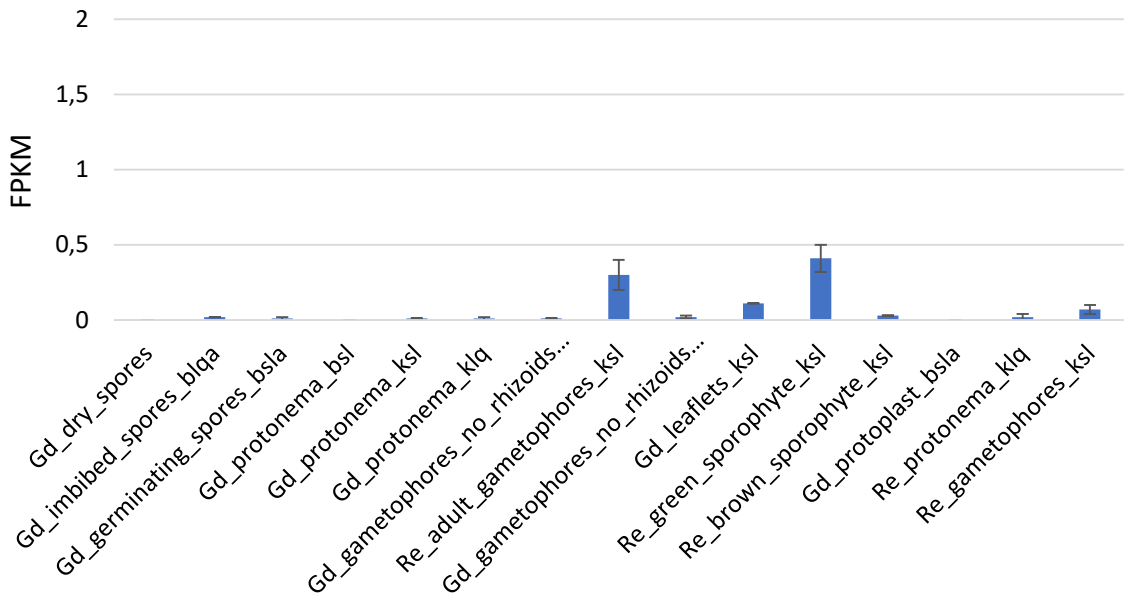

Figure S16: ccdc39 RNA-seq expression throughout different developmental stages. In all libraries ccdc39 expression is below 0.5 FPKM (fragments per kilobase per million reads mapped) whereas genes are defined as expressed with a FPKM equal or above 2. Data from Fernandez-Pozo *et al.*, 2019. Error bars = +/- standard deviation.

Supplemental references

Fernandez-Pozo N, Haas FB, Meyberg R, Ullrich KK, Hiss M, Perroud PF, Hanke S, Kratz V, Powell AF, Vesty EF, Daum CG, Zane M, Lipzen A, Sreedasyam A, Grimwood J, Coates JC, Barry K, Schmutz J, Mueller LA, Rensing SA (2019). PEATmoss (Physcomitrella Expression Atlas Tool): a unified gene expression atlas for the model plant *Physcomitrella patens Plant J*.

Ortiz-Ramirez C, Hernandez-Coronado M, Thamm A, Catarino B, Wang M, Dolan L, Feijo JA, Becker JD (2016). A Transcriptome Atlas of Physcomitrella patens Provides Insights into the Evolution and Development of Land Plants. *Mol Plant* **9**(2): 205-220.